# Brain image-derived phenotypes yield insights into causal risk of psychiatric disorders using a Mendelian randomization study

Jing Guo[1], Ke Yu[1], Yan Guo[1], Shi Yao[1], Hao Wu[1], Kun Zhang[1], Yu Rong[1], Ming-Rui Guo[1], Shan-Shan Dong[1], Tie-Lin Yang[1*]

[1]Key Laboratory of Biomedical Information Engineering of Ministry of Education, Biomedical Informatics & Genomics Center, School of Life Science and Technology, Xi'an Jiaotong University, Xi'an, Shaanxi, P. R. China, 710049

**Running title:** Causal IDPs in Psychiatric Disorders

*Corresponding author: Tie-Lin Yang, Ph.D.

Key Laboratory of Biomedical Information Engineering of Ministry of Education, Biomedical Informatics & Genomics Center, School of Life Science and Technology, Xi'an Jiaotong University, Xi'an, Shaanxi, P. R. China, 710049

Email: yangtielin@xjtu.edu.cn

Total words = 2034 Words (not including title page, methods and figure legends).

Abstract =148

Introduction=407

Results = 966

Discussion= 418

Conclusion = 95

Method = 1072

**Abstract**

Brain imaging-derived phenotypes (IDPs) serve as underlying functional intermediates in psychiatric disorders, both of which are highly polygenic and heritable. Observational studies have elucidated the correlation between IDPs and psychiatric disorders, yet no systematic screening of IDPs to confer the causal liability in such disorders. We conducted a two-sample Mendelian randomization framework to explore the causality of 1,345 IDPs on 10 psychiatric disorders and established the BrainMR database (http://brainmr.online/idp2psy/Index.php). We identified 73 pairs with causality and rigorously examined them through various sensitivity analyses, 26 of which were completely novel. The top significant causality was the volume of right Heschl's gyrus, which increased the risk of major depressive disorder with an estimated OR of 1.13 (95% CI 1.07-1.19, $P = 7.69\times10^{-6}$). We also illustrated that the causal IDPs were specific to psychiatric disorders. Overall, our study provides unique insights into causal pathways of psychiatric disorders at the imaging levels.

Key Words:

Psychiatric disorders, IDPs, Causality, Mendelian Randomization

## Introduction

Psychiatric disorders are a group of serious brain dysfunction illnesses in which individuals are disturbed emotionally, cognitively or behaviorally. Millions of people worldwide are reported to suffer from psychiatric disorders, which are the main cause of disability and social burdens, and are therefore considered serious public health problems[1,2].

Psychiatric disorders can be characterized by a collection of physiological brain changes, including many heritable image-derived phenotypes (IDPs) that can be measured non-invasively using magnetic resonance imaging (MRI)[3-6]. IDPs could serve as intermediate phenotypes and effective indicators of risk factors for psychiatric disorders[7]. A large number of observational studies have been performed to explore the relationship between IDPs and psychiatric disorders. For example, the smaller cortical thicknesses of the insula and rostral anterior cingulate cortex are regarded as cerebral markers for adolescent anxiety[8]. The FA values of left superior longitudinal fasciculus, left prefrontal cortex, and left parietal lobe in patients with major depressive disorder (MDD) are lower than those in controls[9]. The thicknesses of the temporal and parietal cortex are decreased in patients with schizophrenia[10], whereas increased in patients with autism spectrum disorder (ASD)[11]. However, single brain IDP may not accurately reflect the state of the disease in most cases, multiple IDPs are needed as diagnostic reference. Moreover, findings from conventional observational studies could not account for confounding factors. It is critical to explore the causal relationships between IDPs and psychiatric disorders.

Mendel randomization (MR) is a widely used epidemiological method that uses genetic variants as instrument to infer the causality between exposure factors and outcomes[12,13]. With the accomplishment of the genome-wide association study (GWAS) on IDPs[3,14], it provides us with the opportunity to systematically explore the causal relationships between all the IDPs and psychiatric disorders using large-scale data. Therefore, in this study, we performed an optimized two-sample MR framework to estimate causal risk factors for psychiatric disorders at brain IDPs levels. First, we systematically screened the causal effects of a total of 1,345 IDPs as exposures (including 670 structural MRI and 675 diffusion MRI, respectively), on 10 psychiatric disorders as outcomes in ~8,428 UK Biobank participants. Second, we assessed the commonality and specificity of brain IDPs, which could explain their wide-ranging effects in psychopathology. Finally, we established a BrainMR database (http://brainmr.online/idp2psy/Index.php) to provide a useful resource to share our results. Our findings could offer a systemic view of the causal effects of IDPs and psychiatric disorders. The identified IDPs may be applied as potential targets for etiology diagnosis.

## Results

### Overview of causality framework between IDPs and psychiatric disorders

We used an optimized two-sample MR pipeline to assess the causal associations between 1,345 IDPs and 10 psychiatric disorders by using the GWAS summary-level data. The detailed information of all the GWAS statistics is summarized in Supplementary Tables 1-2. The flowchart of our analyses is shown in Figure 1.

We applied strict pipeline to select qualified instrument variants (IVs). Firstly, we removed a total of 4369 IVs, which were associated with confounders related to exposures or outcomes (Figure 2a and Supplementary Table 3). Most of these confounders related to exposures were mainly affected by body mass index and alcohol intake frequency. For the confounders related to outcomes, we conducted genetic correlation analyses of 48 brain traits (Supplementary Figure 1a). Among them, MDD had the largest number of 11 confounders, and neuroticism was a common confounder affecting psychiatric outcomes except for PTSD (Supplementary Figure 1b). Second, we discarded 399 IVs that had direct or indirect LD effect with variants of outcomes (Supplementary Table 4). Next, we conducted heterogeneity test and removed 11,394 outliers (Supplementary Table 5). We excluded 872 exposure-outcome pairs that did not meet the requirements of F-statistics or minimum number of IVs (Figure 2b-c and Supplementary Table 6). After above screening, we found that the effective IVs selected from IDPs were apparent different from those in psychiatric disorders (Supplementary Figure 2a-b).

**Sensitivity analyses corrected the causal effects on the main MR results**

We applied inverse-variance weighted (IVW) analysis as the primary method to estimate causal effects of each IDP on each of psychiatric disorders. Since the majority of IDPs were genetically correlated with each other (Figure 2b-c), we set the significance threshold as 0.005 for MR analyses[15,16] to avoid overly multiple testing adjustment. Therefore, across 1,345 IDPs, we preliminary identified 85 statistically significant causal relationships through IVW method (full results shown in Supplementary Table 7).

In order to ensure the robustness of MR results, we performed sensitivity analyses. First, we conducted

leave-one-out cross-validation, and found that only one pair had non-significant causality at the nominal *p*-value of 0.05 (corpus callosum (IDP.0535) on ADHD after removing rs947787) (Supplementary Figure 3). Second, we performed global test of MR-PRESSO to examine horizontal pleiotropic outlier and found 12 pairs for potential horizontal pleiotropy with *p*-value less than 0.05. We corrected the IVW analyses after removing pleiotropic outliers, but 4 pairs were still not significant ($P > 0.005$) (Supplementary Figure 4a). Third, five pairs were disputed with directional pleiotropy based on the MR-Egger regression analyses, whose intercepts were significantly deviated from zero (Supplementary Figure 4b). Fourth, we carried out reverse causal inference and found that there were three reverse causal associations in our MR results (Supplementary Figure 4c), suggesting that the directionality of these three causal relationships was questionable. Taken together, we excluded a total of 12 pairs through sensitivity analyses (Supplementary Figure 4d).

**Identification of causal IDPs in psychiatric disorders**

After removing the unqualified pairs in the sensitivity analyses, 73 pairs were identified as effective causal relationships (Figure 3). There were more than one causal IDP for each of the psychiatric disorders, and the numbers of causal IDPs from high to low involved in disorders were ADHD (13), MDD (11), PTSD (9), obsessive compulsive disorder (OCD) (8), anxiety (7), schizophrenia (7), bipolar disorder (6), autism spectrum disorder (ASD) (5), Tourette syndrome (4) and anorexia nervosa (3). Among them, the *p*-value of significant causality was ranged from $7.69 \times 10^{-6}$ to $4.81 \times 10^{-3}$, and the OR of estimation was ranged from 0.54 to 1.87. ADHD was detected with the largest number of causal IDPs, including 7 positive causalities and 6 negative causalities. The top significant causal relationship was a unit higher volume of right Heschl's gyrus (IDP.0115), which was causally associated with an

increased MDD risk with an estimated OR of 1.13 (95% CI 1.07-1.19, $P = 7.69 \times 10^{-6}$).

We used another three MR approaches, including MR-Egger regression, weighted median-based MR and mode-based MR to validate our results of IVW method. We identified that 76.7% (56/73) of the causal pairs were successfully validated by any of these three methods (normal $p$-value < 0.05), and the directions of causation were consistent with IVW-MR results (Figure 4a-b).

All of our results of causality between brain IDPs and psychiatric disorders were integrated into an open online BrainMR database (http://brainmr.online/idp2psy/Index.php) for public access. All the raw data in the BrianMR database have been uniformly stored, so as to facilitate rapid and systematic queries.

**Causal IDPs are specific to psychiatric disorders**

According to the anatomical classification, IDPs of brain structure MRI were divided into eight regions including frontal lobe, parietal lobe, temporal lobe, occipital lobe, insular lobe, cerebellum, hippocampus and other scattered regions (Figure 5a), while IDPs of diffusion MRI were divided into four types of structural connectivity, including projection fibers, association fibers, commissural fibers and brainstem tracts (Figure 5b). We found that each psychiatric disorder had multiple IDPs as risk factors, however, there was almost no overlap among them except only two IDPs. One was the volume of right hippocampus (IDP.2682), which was the causal inducer both for MDD and PTSD (Figure 5a), the other was OD value of right tract of para-hippocampal in cingulum (IDP.0824), which was the causal inducer both for MDD and OCD (Figure 5b).

We found that most of the psychiatric disorders were genetically correlated with each other, accounting for 35.6% in 45 pairs (Figure 5c). However, most of the causal IDPs in psychiatric disorders were independent of each other, only 1.4% of causal IDPs were genetically correlated (Figure 5c). Through hierarchical clustering analysis, we divided psychiatric disorders into two categories (Figure 5c). There was no overlapping IDP between these two clusters. Therefore, we preliminarily speculated that the psychiatric disorders might be specific at the level of brain imaging.

## Discussion

In this study, we performed two-sample MR analyses to systematically investigate the causal effects of 1,345 IDPs on 10 psychiatric disorders, with large GWAS statistics from UK biobank and PGC database. Most of the previous studies were based on imaging data from case-control groups, which was limited by the sample size, high economic cost, and especially lack of causal reasoning. In addition, the types of imaging data reported in previous studies were relatively limited. We identified a total of 73 pairs of causal IDPs on psychiatric disorders, which could be used to prioritize promising biomarkers for predicting the risk of psychiatric disorders.

Among the 73 causal pairs we identified between IDPs and psychiatric disorders, we checked previously published literatures and found that 26 pairs were novel causal relationships, 18 pairs had been reported by previous observational studies, and 29 pairs were supported by some indirect evidence (Supplementary Table 8). It's noteworthy that some of our results are supported by effective

association evidences with same direction. For instance, we found that the thickness of left pars-opercularis (IDP.2942) was causally associated with decreased ADHD risk with an estimated OR of 0.82. It has been supported by a study that the children with ADHD have cortical thinning of the left pars-opercularis[17,18]. The volume of cerebellum vermis and right crus II (IDP.0148 and IDP.0149) were decreased in ADHD patients, and patients with ADHD were also along with the cerebellum diseases[19-21]. The thickness of anterior segment of circular insula (IDP.3111) was causally associated with decreased anxiety from our results, and it has been previously observed from other studies that the smaller thickness of the insula in anxiety[8,22]. On the other hand, some of our causality findings were complementary to the previous observation studies. For example, IDP.3113 is the thickness of right superior segment of the insula that was causally associated with a decreased AN risk. The insula was related to a brain circuit that integrates taste perception, food reward value and cognitive-emotional associations with food[23-26], which could be an indirect evidence of our finding.

Our findings suggest that IDP has a specific effect on the psychiatric disorder, which is unlike the similar polygenic overlap shared among these diseases. A causal IDP might be related to one disease, which indicated an important risk factor leading to the occurrence of this disease. Moreover, there are multiple IDPs causally associated with the same psychiatric disorder. We could integrate multiple IDPs as risk evaluation indicators for pathological occurrence, which could provid theoretical support for disease prediction and diagnosis.

## Conclusion

In summary, we reported the causal brain imaging-derived phenotypes on ten psychiatric disorders through two-sample MR analyses. We identified 26 novel causal IDP-psychiatric disorder pairs, 29 novel causal relationships with indirect evidence, and 18 causalities supported by previous studies. Our results indicate that each psychiatric disorder has its specific causal IDPs. We also develop an open database BrainMR to facilitate quick query between causal IDPs and psychiatric disorders. Taken together, our findings suggest that brain structure and connectivity causally affect brain disorders and could serve as specific risk predictions for early intervention of psychiatric disorders.

## Online Methods

### Data sets

*Exposure data - brain IDPs*

1,345 IDPs were selected as exposures, which were divided into two categories including brain structure (structure MRI) and brain structural connectivity (diffusion MRI) and each was in up to 8,428 European adults. Brain structure included 670 anatomical subtypes such as volume, superficial area and subcortical thickness. Brain structural connectivity included 675 subtypes of long-range structural connectivity and local microstructure with a series of orientation signals by diffusion-weighted imaging (dMRI). The detailed information is provided by UK Biobank online refs (https://biobank.ctsu.ox.ac.uk/crystal/crystal/docs/brain_mri.pdf). Briefly, original IDPs of brain structure were T1 or T2 weighted structural images[27], and different algorithms or methods were performed to generate new image features. Brain structural connectivity IDPs were initially screened by dMRI that was a technique to detect water molecules diffusion with a range of orientations within

local region[28]. All GWAS summary statistics of IDPs were collected from the Oxford BIG web browser (http://big.stats.ox.ac.uk/)[3].

*Outcome data - psychiatric disorders*

We collected ten psychiatric disorders with publicly available GWAS summary statistics as outcomes, namely ADHD[29], anorexia nervosa[30], ASD[31], bipolar disorder[32], MDD[33], OCD[34], PSTD[35], schizophrenia[36], Tourette syndrome[37] and anxiety[38]. The vast majority of these data were derived from Psychiatric Genomics Consortium (PGC)[39]. Individuals used in outcomes were independent of exposures, including 177,545 cases and 317,703 controls of European ancestry in total. The detailed information is summarized in Supplementary Table 2.

*Harmonized process of datasets*

To guarantee the precise causal inference, we conducted harmonization process of original GWAS statistics, which could check whether the SNP alleles were coded from the same strand of DNA[40]. We took genomic reference of 50,000 Europeans from UK Biobank for allele matching. The minor alleles were defined as the effect alleles, which were matched to reference genomes to ensure uniformity of effect direction. Moreover, we checked for palindromic SNPs whose alleles correspond to nucleotides that pairs in forward and reverse coding, such as A/T and G/C. We discarded SNPs if their minor allele frequencies (MAFs) were close to 0.50 (e.g., 0.48 - 0.52), which might introduce ambiguity into the conformity of the effect allele between the exposure and outcome datasets[41]. About 0.20% - 0.47% palindromic SNPs were deleted (Supplementary Table 9).

240 **MR Analysis**

241 *Selection of instrument variants*

242 Firstly, conditional independent SNPs of each IDP were clumped by using PLINK with a stepwise
243 model-selection procedure[42]. We set linkage disequilibrium (LD) pruning $r^2$ threshold = 0.05 in UK
244 Biobank reference, window size = 1 Mb and *p*-value threshold = $1 \times 10^{-5}$. Then, IVs should be
245 associated with target IDP exclusively and not associated with other IDPs in one category (brain
246 structure or connection) to precluded pleiotropic variants. IVs should satisfy three assumptions of
247 conventional MR principle, that is, it must be statistically significant associated with exposure, but not
248 associated with any confounder, and not associated with outcome. We also excluded the variants whose
249 LD was directly or indirectly related to outcome variants with the option (*p*-value $< 5 \times 10^{-8}$ and $r^2 >$
250 0.8). We set p-value $< 1 \times 10^{-5}$ in the step of calculating conditional independent SNPs as IVs
251 (Supplementary Figure 5a-b).

252

253 *Removing confounders*

254 In order to minimize pleiotropy, we removed the multiple IVs associated with confounders. We used
255 PhenoScanner GWAS database (http://www.phenoscanner.medschl.cam.ac.uk/) and NHGRI-EBI
256 GWAS catalog (https://www.ebi.ac.uk/gwas/) to assess any previous associations with confounders.
257 We defined correlated traits as the confounders of designated outcome through genetic correlation
258 between outcomes and 48 brain related traits (summarized in Supplementary Table 10) through LD
259 score regression (LDSC)[43]. We also excluded confounder IVs directly associated with lifestyle and
260 physical factors that affect exposures or outcomes such as alcohol intake[44], smoking[45] and body mass
261 index[46], because these factors could affect brain imaging phenotypes.

*Quality control of instrument variants*

In order to improve the accuracy and robustness of genetic instruments, we proposed heterogeneity test to detect outliers and adjusting them. We used Cochran's Q test for Inverse variance weighted (IVW) model fit in the condition of horizontal pleiotropic influences and exploited Rucker's Q' test for MR-Egger fit by reason of directional pleiotropic influences[47,48]. We implemented the RadialMR version 0.4 R package to calculate the modified Q and Q' test[49], and discarded the statistically significant outliers at the nominal significance level of 0.05. Additionally, we performed fist-stage F-statistics to measure the power of the final genetic instruments, of which lower F statistics correspond to greater bias[50]. We set a conventional threshold of 10 that meaning a qualified IVs set and weak instrument bias is unlikely to occur in MR analysis. We also discarded the exposure-outcome MR test when the number of IVs less than five.

*Two-sample MR Analyses*

We performed two-sample MR analyses to explore the causal relationships between brain IDPs and psychiatric disorders with the valid IVs. Inverse variance weighted (IVW) regression was conducted as the primary causal infere[51]. Since IVW might be biased if any of the SNPs exhibit horizontal pleiotropy, we applied other MR analysis as complementary methods to strengthen the confidence. MR-Egger method estimates the causal effect by slope coefficient of Egger regression, which can provide a more robust estimate even when all genetic variants are invalid IVs[52]. Weighted median-based estimator could offer protection against even up to 50% invalid IVs[53]. Mode-based method provides a consistent estimator when relaxed IV assumptions with less bias and lower type-I error

rates[54]. All these methods were implemented in the TwoSampleMR version 0.4.10 R package[55].

*Sensitivity Analyses*

For outcomes with significant MR analysis results, we conducted sensitivity analyses. First, we executed a leave-one-out cross-validation analysis to check whether causal association was driven by a single SNP. Second, we conducted MR-PRESSO (Mendelian randomization pleiotropy residual sum and outlier) test to detect whether there was any horizontal pleiotropic outlier in our MR study[56]. *P* value less than 0.05 was regarded as an outlier in the statistical significance test. Third, we performed MR-Egger regression to check for potential bias from directional pleiotropy [53]. The intercept in the Egger regression represents the average pleiotropic effect of all genetic variants, and is interpreted as evidence of directed pleiotropy when the value differs from zero. Fourth, to guard against the small possibility that our results were driven by reverse causality, we performed IVW analyses in reverse direction to examine the possible reverse causation bias from psychiatric disorders to IDPs. In this study, we conducted MR in accordance with Strengthening the Reporting of Observational Studies in Epidemiology (STROBE) and STROBE-MR guidelines[57].

## Data availability

The full GWAS summary-level data of brain IDPs were collected from Oxford BIG web browser (version 2.0) through http://big.stats.ox.ac.uk/download_page. GWAS summary statistics of ADHD, AN, ANX, ASD, BD, MDD, OCD, PTSD and TS from PGC are available on the Psychiatric Genomics Consortium's downloads page (https://www.med.unc.edu/pgc/download-results). SCZ was collected from CLOZUK and PGC2 meta-analysis summary statistics through https://walters.psycm.cf.ac.uk. The genome reference for 50,000 Europeans was calculated in house by using genotype data from UK Biobank (https://biobank.ctsu.ox.ac.uk). Summary statistics of the rest of the analyzed traits for condounders removing analyses are available at GRASP (https://grasp.nhlbi.nih.gov/FullResults.aspx), or Gene ATLAS (http://geneatlas.roslin.ed.ac.uk/downloads), or CNCR (https://ctg.cncr.nl/software/summary_statistics), or CCACE (https://www.ccace.ed.ac.uk/node/335), or epiGAD (http://www.epigad.org/gwas_ilae2014), or CDKP (https://cd.hugeamp.org/downloads.html), or http://cnsgenomics.com, or GIANT (http://portals.broadinstitute.org/collaboration/giant/index.php/GIANT_consortium_data_files).

## Code availability

LD-based result clumping was performed using PLINK 1.9 (https://www.cog-genomics.org/plink/1.9/). Genetic correlation analysis was performed using LDSC (https://github.com/bulik/ldsc). R version 3.3.2 (https://www.r-project.org/) was used for statistical

analysis. The TwoSampleMR v0.4.10 R package (https://mrcieu.github.io/TwoSampleMR/), RadialMR v0.4 (https://github.com/WSpiller/RadialMR/) and MR-PRESSO (https://github.com/rondolab/MR-PRESSO) were used for MR analyses. PhenoScanner GWAS database (http://www.phenoscanner.medschl.cam.ac.uk) and NHGRI-EBI GWAS catalog (https://www.ebi.ac.uk/gwas/) were used to remove confounding factors.

**Acknowledgements**

This work was supported by grants from the National Natural Science Foundation of China (31871264, 31970569), the Natural Science Basic Research Program Shaanxi Province (2019JM-119) and the Fundamental Research Funds for the Central Universities. We would like to thank the UK Biobank and Cross-Disorder Group of the Psychiatric Genomics Consortium (PGC).

**Author contributions**

T.L.Y. conceived and supervised this project. J.G. conducted the computational work and wrote the manuscript. K.Y built the website of database. Y.G. revised the manuscript. S.Y and other authors offered some advices and assistances.

**Conflict of Interest**

All the authors declare that they have no conflicts of interest.

## References


1 Disease, G. B. D., Injury, I. & Prevalence, C. Global, regional, and national incidence, prevalence, and years lived with disability for 328 diseases and injuries for 195 countries, 1990-2016: a systematic analysis for the Global Burden of Disease Study 2016. *Lancet* **390**, 1211-1259, doi:10.1016/S0140-6736(17)32154-2 (2017).

2 Charlson, F. *et al.* New WHO prevalence estimates of mental disorders in conflict settings: a systematic review and meta-analysis. *Lancet* **394**, 240-248, doi:10.1016/S0140-6736(19)30934-1 (2019).

3 Elliott, L. T. *et al.* Genome-wide association studies of brain imaging phenotypes in UK Biobank. *Nature* **562**, 210-216, doi:10.1038/s41586-018-0571-7 (2018).

4 Miller, K. L. *et al.* Multimodal population brain imaging in the UK Biobank prospective epidemiological study. *Nat Neurosci* **19**, 1523-1536, doi:10.1038/nn.4393 (2016).

5 Dazzan, P. *et al.* Magnetic resonance imaging and the prediction of outcome in first-episode schizophrenia: a review of current evidence and directions for future research. *Schizophr Bull* **41**, 574-583, doi:10.1093/schbul/sbv024 (2015).

6 Xia, M. & He, Y. Magnetic resonance imaging and graph theoretical analysis of complex brain networks in neuropsychiatric disorders. *Brain Connect* **1**, 349-365, doi:10.1089/brain.2011.0062 (2011).

7 Meyer-Lindenberg, A. & Weinberger, D. R. Intermediate phenotypes and genetic mechanisms of psychiatric disorders. *Nat Rev Neurosci* **7**, 818-827, doi:10.1038/nrn1993 (2006).

8 Suffren, S., Chauret, M., Nassim, M., Lepore, F. & Maheu, F. S. On a continuum to anxiety disorders: Adolescents at parental risk for anxiety show smaller rostral anterior cingulate cortex and insula thickness. *J Affect Disord* **248**, 34-41, doi:10.1016/j.jad.2019.01.028 (2019).

9 Srivastava, S., Bhatia, M. S., Bhargava, S. K., Kumari, R. & Chandra, S. A Diffusion Tensor Imaging Study Using a Voxel-Based Analysis, Region-of-Interest Method to Analyze White Matter Abnormalities in First-Episode, Treatment-Naive Major Depressive Disorder. *J Neuropsychiatry Clin Neurosci* **28**, 131-137, doi:10.1176/appi.neuropsych.15050120 (2016).

10 Rimol, L. M. *et al.* Cortical thickness and subcortical volumes in schizophrenia and bipolar disorder. *Biol Psychiatry* **68**, 41-50, doi:10.1016/j.biopsych.2010.03.036 (2010).

11 Hardan, A. Y., Muddasani, S., Vemulapalli, M., Keshavan, M. S. & Minshew, N. J. An MRI study of increased cortical thickness in autism. *Am J Psychiatry* **163**, 1290-1292, doi:10.1176/ajp.2006.163.7.1290 (2006).

12 Smith, G. D. & Ebrahim, S. 'Mendelian randomization': can genetic epidemiology contribute to understanding environmental determinants of disease? *Int J Epidemiol* **32**, 1-22, doi:10.1093/ije/dyg070 (2003).

13 Davey Smith, G. & Hemani, G. Mendelian randomization: genetic anchors for causal inference in epidemiological studies. *Hum Mol Genet* **23**, R89-98, doi:10.1093/hmg/ddu328 (2014).

14 Satizabal, C. L. *et al.* Genetic architecture of subcortical brain structures in 38,851 individuals. *Nat Genet* **51**, 1624-1636, doi:10.1038/s41588-019-0511-y (2019).

15 Benjamin, D. J. *et al.* Redefine statistical significance. *Nat Hum Behav* **2**, 6-10, doi:10.1038/s41562-017-0189-z (2018).

16 Ioannidis, J. P. A. The Proposal to Lower P Value Thresholds to .005. *JAMA* **319**, 1429-1430, doi:10.1001/jama.2018.1536 (2018).

17 Liu, T., Chen, Y., Li, C., Li, Y. & Wang, J. Altered brain structural networks in attention deficit/hyperactivity disorder children revealed by cortical thickness. *Oncotarget* **8**, 44785-44799, doi:10.18632/oncotarget.14734 (2017).

18 Batty, M. J. *et al.* Cortical gray matter in attention-deficit/hyperactivity disorder: a structural magnetic resonance imaging study. *J Am Acad Child Adolesc Psychiatry* **49**, 229-238, doi:10.1016/j.jaac.2009.11.008

(2010).

19 Curtin, K. *et al.* Increased risk of diseases of the basal ganglia and cerebellum in patients with a history of attention-deficit/hyperactivity disorder. *Neuropsychopharmacology* **43**, 2548-2555, doi:10.1038/s41386-018-0207-5 (2018).

20 Seidman, L. J. *et al.* Gray matter alterations in adults with attention-deficit/hyperactivity disorder identified by voxel based morphometry. *Biol Psychiatry* **69**, 857-866, doi:10.1016/j.biopsych.2010.09.053 (2011).

21 Wyciszkiewicz, A., Pawlak, M. A. & Krawiec, K. Cerebellar Volume in Children With Attention-Deficit Hyperactivity Disorder (ADHD). *J Child Neurol* **32**, 215-221, doi:10.1177/0883073816678550 (2017).

22 Syal, S. *et al.* Grey matter abnormalities in social anxiety disorder: a pilot study. *Metab Brain Dis* **27**, 299-309, doi:10.1007/s11011-012-9299-5 (2012).

23 Frank, G. K., Shott, M. E., Riederer, J. & Pryor, T. L. Altered structural and effective connectivity in anorexia and bulimia nervosa in circuits that regulate energy and reward homeostasis. *Transl Psychiatry* **6**, e932, doi:10.1038/tp.2016.199 (2016).

24 Kim, K. R., Ku, J., Lee, J. H., Lee, H. & Jung, Y. C. Functional and effective connectivity of anterior insula in anorexia nervosa and bulimia nervosa. *Neurosci Lett* **521**, 152-157, doi:10.1016/j.neulet.2012.05.075 (2012).

25 Pfuhl, G. *et al.* Preserved white matter microstructure in young patients with anorexia nervosa? *Hum Brain Mapp* **37**, 4069-4083, doi:10.1002/hbm.23296 (2016).

26 Shott, M. E., Pryor, T. L., Yang, T. T. & Frank, G. K. Greater Insula White Matter Fiber Connectivity in Women Recovered from Anorexia Nervosa. *Neuropsychopharmacology* **41**, 498-507, doi:10.1038/npp.2015.172 (2016).

27 Zhang, Y., Brady, M. & Smith, S. Segmentation of brain MR images through a hidden Markov random field model and the expectation-maximization algorithm. *IEEE Trans Med Imaging* **20**, 45-57, doi:10.1109/42.906424 (2001).

28 Sotiropoulos, S. N. *et al.* Advances in diffusion MRI acquisition and processing in the Human Connectome Project. *Neuroimage* **80**, 125-143, doi:10.1016/j.neuroimage.2013.05.057 (2013).

29 Martin, J. *et al.* A Genetic Investigation of Sex Bias in the Prevalence of Attention-Deficit/Hyperactivity Disorder. *Biol Psychiatry* **83**, 1044-1053, doi:10.1016/j.biopsych.2017.11.026 (2018).

30 Duncan, L. *et al.* Significant Locus and Metabolic Genetic Correlations Revealed in Genome-Wide Association Study of Anorexia Nervosa. *Am J Psychiatry* **174**, 850-858, doi:10.1176/appi.ajp.2017.16121402 (2017).

31 Grove, J. *et al.* Identification of common genetic risk variants for autism spectrum disorder. *Nat Genet* **51**, 431-444, doi:10.1038/s41588-019-0344-8 (2019).

32 Stahl, E. A. *et al.* Genome-wide association study identifies 30 loci associated with bipolar disorder. *Nat Genet* **51**, 793-803, doi:10.1038/s41588-019-0397-8 (2019).

33 Wray, N. R. *et al.* Genome-wide association analyses identify 44 risk variants and refine the genetic architecture of major depression. *Nat Genet* **50**, 668-681, doi:10.1038/s41588-018-0090-3 (2018).

34 International Obsessive Compulsive Disorder Foundation Genetics, C. & Studies, O. C. D. C. G. A. Revealing the complex genetic architecture of obsessive-compulsive disorder using meta-analysis. *Mol Psychiatry* **23**, 1181-1188, doi:10.1038/mp.2017.154 (2018).

35 Duncan, L. E. *et al.* Largest GWAS of PTSD (N=20 070) yields genetic overlap with schizophrenia and sex differences in heritability. *Mol Psychiatry* **23**, 666-673, doi:10.1038/mp.2017.77 (2018).

36 Pardinas, A. F. *et al.* Common schizophrenia alleles are enriched in mutation-intolerant genes and in regions under strong background selection. *Nat Genet* **50**, 381-389, doi:10.1038/s41588-018-0059-2 (2018).

37 Yu, D. *et al.* Interrogating the Genetic Determinants of Tourette's Syndrome and Other Tic Disorders Through Genome-Wide Association Studies. *Am J Psychiatry* **176**, 217-227, doi:10.1176/appi.ajp.2018.18070857 (2019).

38 Otowa, T. *et al.* Meta-analysis of genome-wide association studies of anxiety disorders. *Mol Psychiatry* **21**, 1391-1399, doi:10.1038/mp.2015.197 (2016).

39 Geschwind, D. H. & Flint, J. Genetics and genomics of psychiatric disease. *Science* **349**, 1489-1494, doi:10.1126/science.aaa8954 (2015).

40 Lawlor, D. A., Harbord, R. M., Sterne, J. A., Timpson, N. & Davey Smith, G. Mendelian randomization: using genes as instruments for making causal inferences in epidemiology. *Stat Med* **27**, 1133-1163, doi:10.1002/sim.3034 (2008).

41 Hartwig, F. P., Davies, N. M., Hemani, G. & Davey Smith, G. Two-sample Mendelian randomization: avoiding the downsides of a powerful, widely applicable but potentially fallible technique. *Int J Epidemiol* **45**, 1717-1726, doi:10.1093/ije/dyx028 (2016).

42 Purcell, S. *et al.* PLINK: a tool set for whole-genome association and population-based linkage analyses. *Am J Hum Genet* **81**, 559-575, doi:10.1086/519795 (2007).

43 Bulik-Sullivan, B. *et al.* An atlas of genetic correlations across human diseases and traits. *Nat Genet* **47**, 1236-1241, doi:10.1038/ng.3406 (2015).

44 Schumann, G. *et al.* KLB is associated with alcohol drinking, and its gene product beta-Klotho is necessary for FGF21 regulation of alcohol preference. *Proc Natl Acad Sci U S A* **113**, 14372-14377, doi:10.1073/pnas.1611243113 (2016).

45 Tobacco & Genetics, C. Genome-wide meta-analyses identify multiple loci associated with smoking behavior. *Nat Genet* **42**, 441-447, doi:10.1038/ng.571 (2010).

46 Yengo, L. *et al.* Meta-analysis of genome-wide association studies for height and body mass index in approximately 700000 individuals of European ancestry. *Hum Mol Genet* **27**, 3641-3649, doi:10.1093/hmg/ddy271 (2018).

47 Greco, M. F., Minelli, C., Sheehan, N. A. & Thompson, J. R. Detecting pleiotropy in Mendelian randomisation studies with summary data and a continuous outcome. *Stat Med* **34**, 2926-2940, doi:10.1002/sim.6522 (2015).

48 Rucker, G., Schwarzer, G., Carpenter, J. R., Binder, H. & Schumacher, M. Treatment-effect estimates adjusted for small-study effects via a limit meta-analysis. *Biostatistics* **12**, 122-142, doi:10.1093/biostatistics/kxq046 (2011).

49 Bowden, J. *et al.* Improving the visualization, interpretation and analysis of two-sample summary data Mendelian randomization via the Radial plot and Radial regression. *Int J Epidemiol* **47**, 2100, doi:10.1093/ije/dyy265 (2018).

50 Zeng, P. & Zhou, X. Causal Association Between Birth Weight and Adult Diseases: Evidence From a Mendelian Randomization Analysis. *Front Genet* **10**, 618, doi:10.3389/fgene.2019.00618 (2019).

51 Burgess, S., Butterworth, A. & Thompson, S. G. Mendelian randomization analysis with multiple genetic variants using summarized data. *Genet Epidemiol* **37**, 658-665, doi:10.1002/gepi.21758 (2013).

52 Bowden, J., Davey Smith, G., Haycock, P. C. & Burgess, S. Consistent Estimation in Mendelian Randomization with Some Invalid Instruments Using a Weighted Median Estimator. *Genet Epidemiol* **40**, 304-314, doi:10.1002/gepi.21965 (2016).

53 Bowden, J., Davey Smith, G. & Burgess, S. Mendelian randomization with invalid instruments: effect estimation and bias detection through Egger regression. *Int J Epidemiol* **44**, 512-525, doi:10.1093/ije/dyv080 (2015).

54 Hartwig, F. P., Davey Smith, G. & Bowden, J. Robust inference in summary data Mendelian randomization via the zero modal pleiotropy assumption. *Int J Epidemiol* **46**, 1985-1998, doi:10.1093/ije/dyx102 (2017).

55 Hemani, G. *et al.* The MR-Base platform supports systematic causal inference across the human phenome. *Elife* **7**, doi:10.7554/eLife.34408 (2018).

56 Verbanck, M., Chen, C. Y., Neale, B. & Do, R. Detection of widespread horizontal pleiotropy in causal relationships inferred from Mendelian randomization between complex traits and diseases. *Nat Genet* **50**, 693-698, doi:10.1038/s41588-018-0099-7 (2018).

57 George Davey Smith, N. M. D., Niki Dimou, Matthias Egger, Valentina Gallo, Robert Golub, Julian PT Higgins, Claudia Langenberg, Elizabeth W Loder, J Brent Richards, Rebecca C Richmond, Veronika W Skrivankova, Sonja A Swanson, Nicholas J Timpson, Anne Tybjaerg-Hansen, Tyler J VanderWeele, Benjamin AR Woolf, James Yarmolinsky. STROBE-MR: guidelines for strengthening the reporting of Mendelian randomization studies. *PeerJ Preprints* **7** (2019).

490 **Figures and legends**

491 **Figure 1**

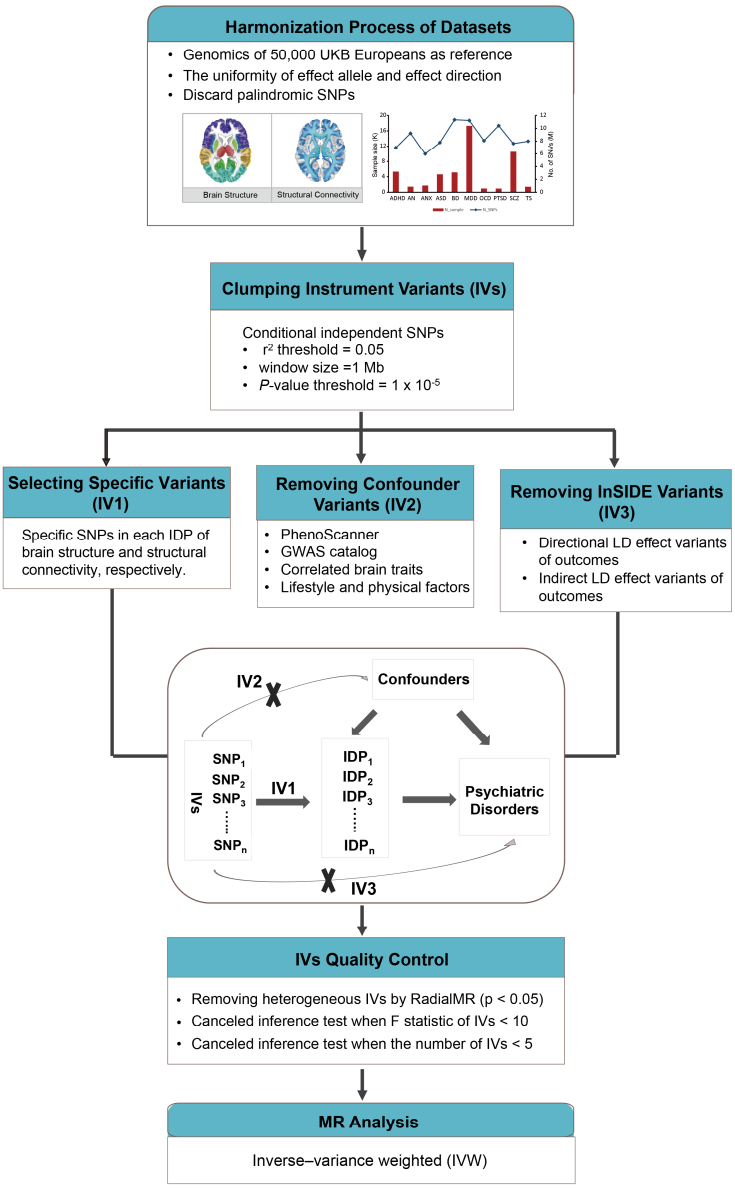


492

493 Workflow of causal inference between IDPs and psychiatric disorders. Abbreviation: attention deficit hyperactivity

494 disorder (ADHD), anorexia nervosa (AN), anxiety disorder (ANX), autism spectrum disorder (ASD), bipolar disorder

495 (BD), major depressive disorder (MDD), obsessive compulsive disorder (OCD), post-traumatic stress disorder

496 (PTSD), schizophrenia (SCZ) and Tourette syndrome (TS).

**Figure 2**

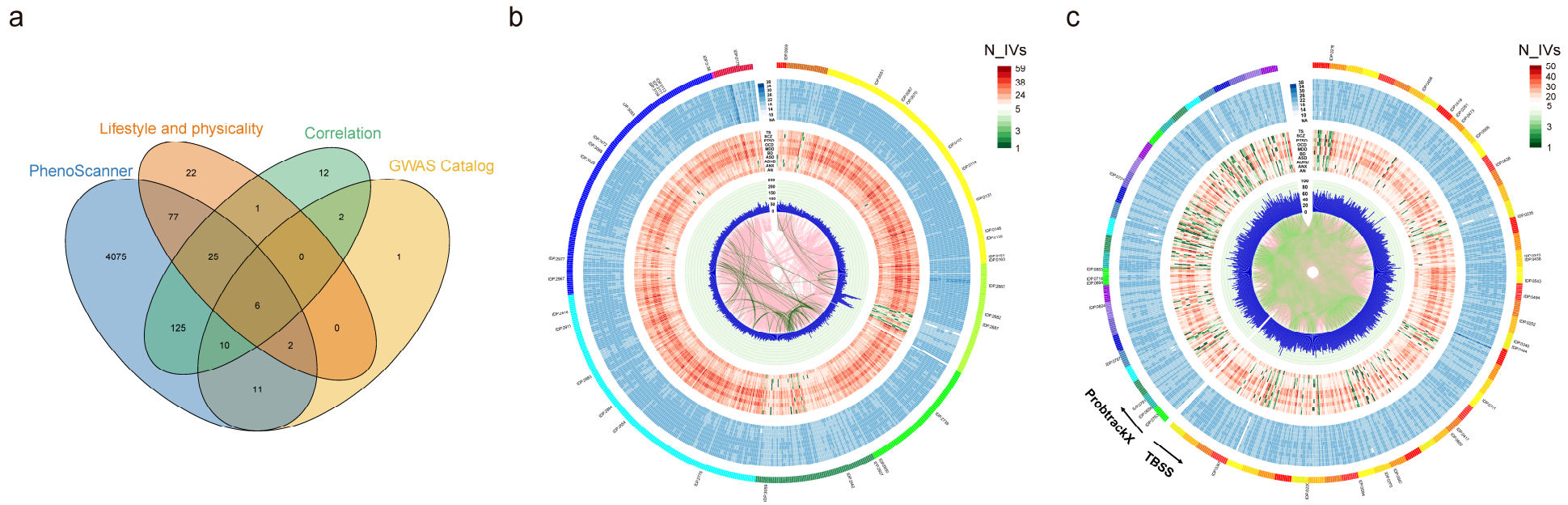


The selection of IVs. (a) Venn diagram shows the number of IVs associated with confounders from four strategies. (b) Circos plots reflect basic information of IVs filtering in brain structure MRI IDPs and (c) brain diffusion MRI IDPs. There are five circles from inside to outside, the inner circle denotes the genetic correlation between each two IDPs, positive with pink and negative with green, the second circle denotes the number of clumping IVs, the third circle denotes the number of final IVs in each exposure-outcome pair, and the fourth circle denotes the F-statistic of IVs in each exposure-outcome pair, and the outer circle denotes the IDPs.

503 **Figure 3**

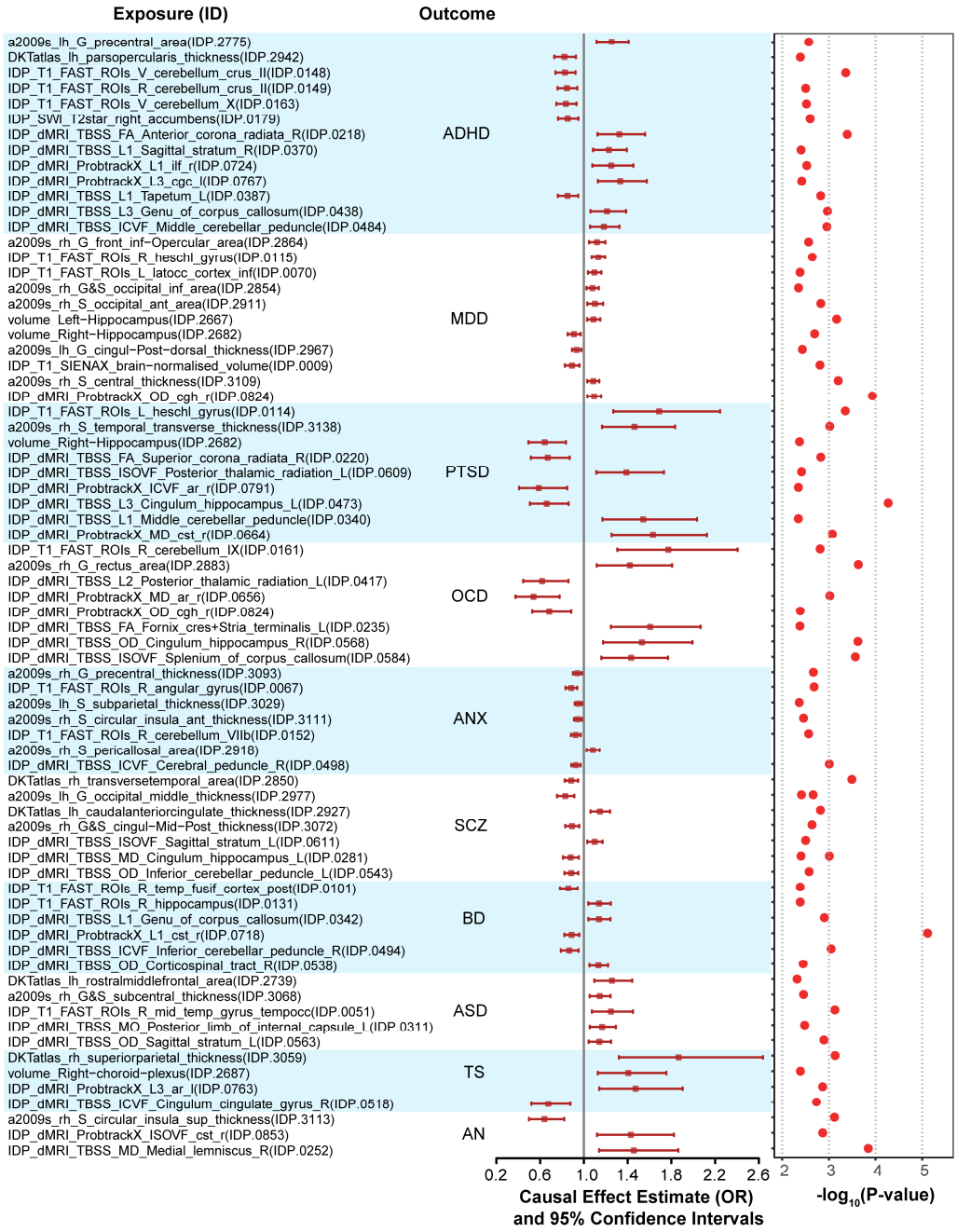


504

505 Mendelian randomization estimates of the causal effect of IDPs on psychiatric disorders using the

506 IVW method. Forest plots show the significant causality with $p$-value < 0.005, and the estimated

507 causal change in odds ratios (OR) with 95% confidence intervals (CI).

**Figure 4**

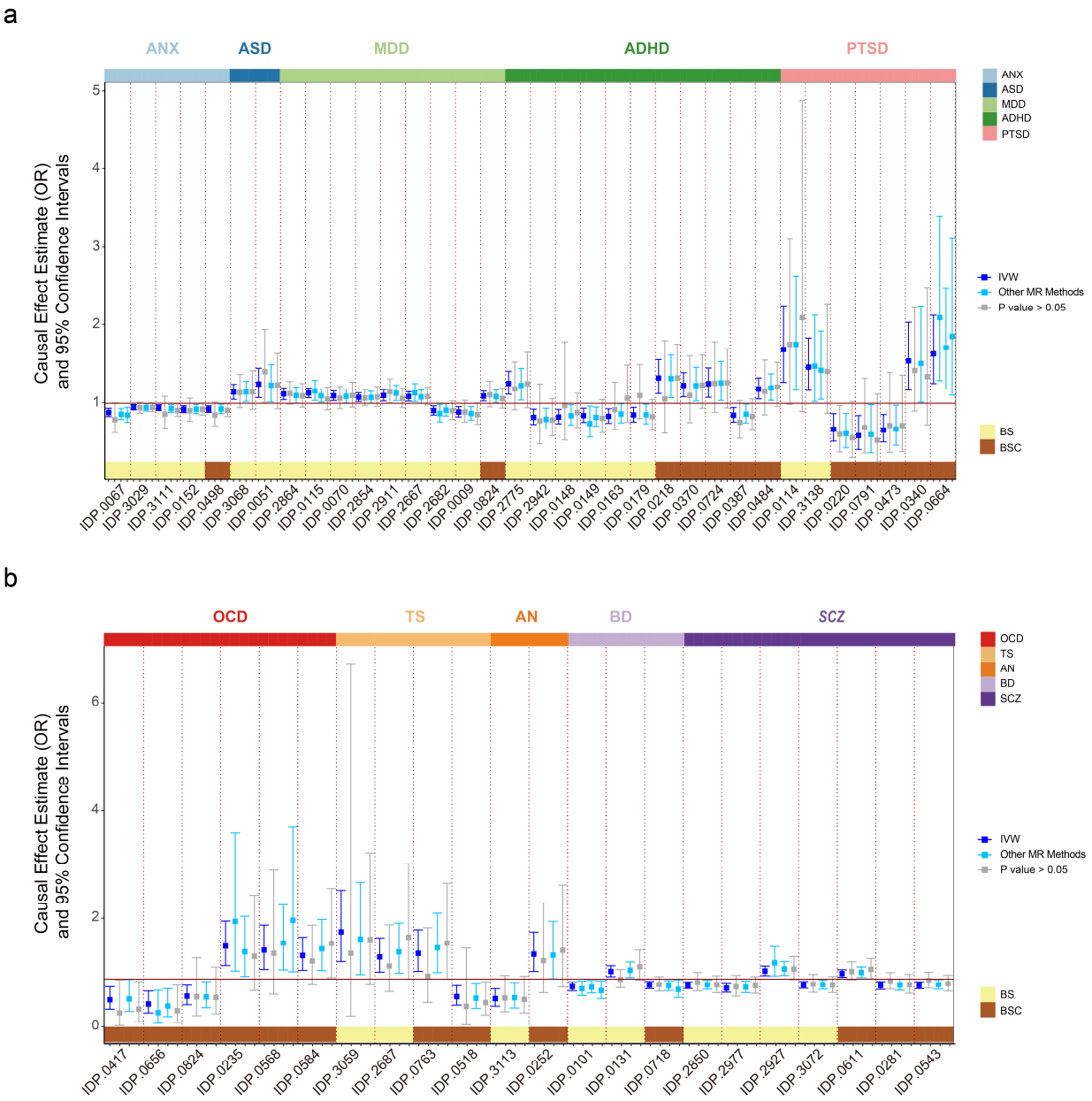


The validation of the causality by other MR approaches. (a-b) Effect estimates (OR) and 95% confidence intervals (CI) of other three MR methods (light blue) compare to IVW (dark blue). From left to right, the box-and-whiskers plot are IVW, MR-Egger slope, weighted median-based MR, and mode-based MR. The gray bars represent *p*-value is greater than 0.05 in corresponding MR approach. Abbreviation: brain structure MRI (BS), brain structural connectivity MRI (BSC).

**Figure 5**

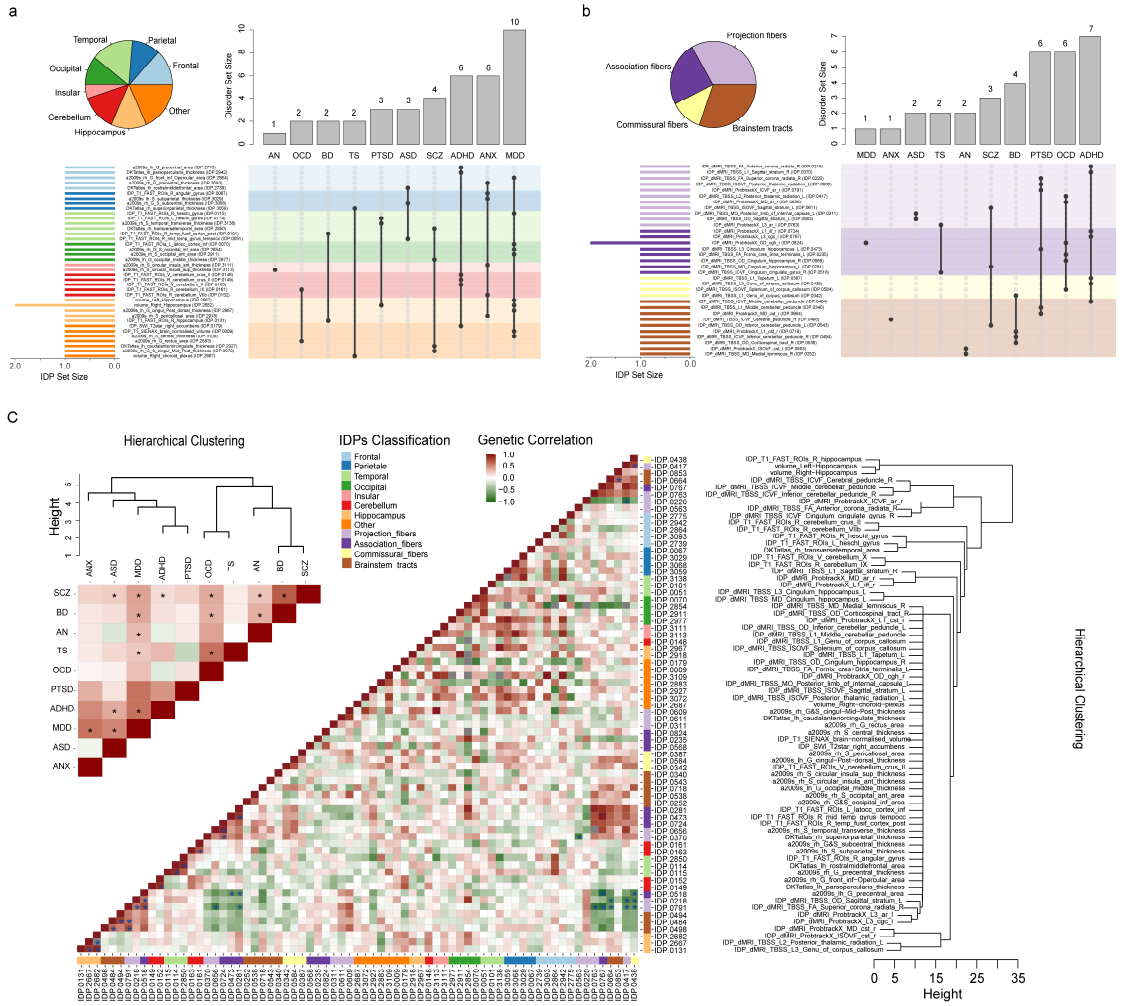


Causal IDPs had specific effects on psychiatric disorders. (a) Causal IDPs of brain structure MRI are divided into different anatomical regions in a pie chart. Bar plot shows the count of causality in each causal IDP or disorder, and black dot represents causal relationship. (b) anatomical classification and the count of causal relationships for causal IDPs of brain diffusion MRI. (c) Genetic correlation and hierarchical clustering for ten psychiatric disorders and causal IDPs, respectively. The symbol of asterisk denotes significance, Bonferroni-adjusted *p*-value threshold are $1\times10^{-4}$ for psychiatric disorders and $6\times10^{-8}$ for IDPs.